

The Impact of User Effects on the Performance of Dual Receive Antenna Diversity Systems in Flat Rayleigh Fading Channels

Peng LIU, Nemanja Stefan PEROVIĆ, Andreas SPRINGER

Institute for Communications Engineering and RF-Systems, Johannes Kepler University
Altenberger Straße 69, 4040 Linz, Austria

{p.liu, n.perovic, a.springer}@nthfs.jku.at

Abstract. *In this paper we study the impact of user effects on the performance of receive antenna diversity systems in flat Rayleigh fading channels. Three diversity combining techniques are compared: maximal ratio combining (MRC), equal gain combining (EGC), and selection combining (SC). User effects are considered in two scenarios: 1) body loss (the reduction of effective antenna gain due to user effects) on a single antenna, and 2) equal body loss on both antennas. The system performance is assessed in terms of mean SNR, link reliability, bit error rate of BPSK, diversity order and ergodic capacity. Our results show that body loss on a single antenna has limited (bounded) impact on system performance. In comparison, body loss on both antennas has unlimited (unbounded) impact and can severely degrade system performance. Our results also show that with increasing body loss on a single antenna the performance of EGC drops faster than that of MRC and SC. When body loss on a single antenna is larger than a certain level, EGC is not a “sub-optimal” method anymore and has worse performance than SC.*

Keywords

Body loss, diversity gain, hand effects, Rayleigh fading, receive antenna diversity, user effects.

1. Introduction

Driven by increasing demands on capacity and data rates, numerous multiple-antenna technologies have been used to improve the wireless system performance [1, 2]. Among many technologies, receive antenna diversity is one that deploys multiple antennas at the receiver side to achieve higher link reliability and increased signal-to-noise ratio (SNR). On one hand, multiple antennas receive more power than a single antenna. On the other hand, because signals transmitted over mobile channels are subject to fading due

to shadowing, multipath, and the Doppler Effect [3], antenna diversity systems also benefit from the fact that the probability of multiple channels being simultaneously in deep fading is significantly lower than the probability of a single channel in deep fading, provided that the antennas are adequately separated such that the channels are largely independent of each other.

In a receive antenna diversity system, signals received from individual branches are usually co-phased and combined before decision. Various diversity combining techniques have been studied tracing back to 1950s. The classic paper by Brennan [4] from that era gives an explanation of the fundamental concepts of the most significant diversity schemes—maximal ratio combining (MRC), equal gain combining (EGC) and selection combining (SC). A lot of other publications have also shown broad applications of receive antenna diversity in modern mobile communication systems – Terrestrial Digital Video Broadcasting (DVB-T) [5], IEEE 802.11 Wireless Local Area Network (WLAN) [6], IEEE 802.16 Worldwide Interoperability for Microwave Access (WiMAX) [7], 3rd Generation Partnership Project (3GPP) Long-Term Evolution (LTE) [8], etc. The vast majority of papers in this topic are looking from a communication link perspective and assume diversity branches with equal gains. However, in practice, diversity branches can have different branch gains. In a system which consists of a main receiver and a secondary receiver, the secondary branch can be differently designed compared to the main branch for functionality, cost or area reasons, giving rise to different branch gains. The gain of mobile antennas can be affected by the user’s body and hand¹ depending on the grip position and the firmness of gripping, which leads to different branch gains. Hence, the assumption that diversity branches are balanced is not always justified.

Because mobile devices operate in the close vicinity of the user’s body, the mobile antenna performance is inevitably affected by the user’s head, hand and torso in terms of radiation pattern, resonance frequency, radiation

¹The affection of the user’s body and hand on the mobile antenna is called “body and hand effects”. Another term “user effects”, which appears in the title of this article, is used exchangeably as a synonym of “body and hand effects”.

efficiency and impedance. References [9–13] have shown that the change of antenna characteristics and degradation of antenna performances due to the user's body (especially hand) is significant. When the mobile antenna is covered by the user's hand, which is the usual case, its radiation efficiency can be reduced by 7–12 dB due to body absorption (dominated by hand). Moreover, due to the body and hand effects, the antenna suffers from impedance mismatch which can introduce an additional reduction in antenna efficiency by 2–4 dB. Despite that the numbers of the reduction in antenna efficiency differ from case to case, a body loss of 7–14 dB is most commonly reported. Experimental results have also shown that, in worst cases, the total loss caused by the user can rise up to 26 dB [13]. These facts imply that there is a need to re-examine the performance of receive antenna diversity systems taking into account the antenna issues. The meaning of such a work is multi-purpose: to more precisely evaluate practical system performance; to provide a basis for antenna impedance matching network design and matching algorithm design [14, 15]; and to help in making trade-offs when the designer has to compromise between minimized user effects (via proper antenna placement) and reduced channel correlation (via giving larger antenna separation).

In this paper, we conduct a study on dual receive antenna diversity systems in flat Rayleigh fading channels. The three aforementioned combining techniques, MRC, EGC, and SC, are considered. The mechanism of how mobile antenna performance is reduced due to body and hand effects is explained. Numbers on reduction of mobile antenna gain are collected across literature to help in developing a quantitative understanding of the issues. Two typical use scenarios of a mobile device, namely a single antenna affected by the user or both antennas affected by the user, are selected for analysis.

We notice [16] which is on the effect of having unequal branch gains in diversity systems. However, because the focus is different the results from that paper do not apply to our problem. In [16], the focus is on unequal branch gains due to imperfect gain tracking in the receiver which affects both the signal power and noise level. In our work, we assume perfect channel knowledge at the receiver. Unequal antenna gains leads to unequal signal powers. The noise level is the same across branches.

The rest of the paper is organized as follows. Section 2 describes the signal and system model. Section 3 explains the mechanism of how mobile antennas are affected by the user and presents collected numbers on body loss. Section 4 lists the figures of merit we use in this paper. In Section 5, we derive closed-form expressions for mean SNR, probability distribution and BER performance of different combining methods involving body loss. In Section 6, we present numerical results on diversity order and ergodic channel capacity, and also give discussions on the impact of user effects. Finally, in Section 7 we give the conclusion.

2. Signal and System Model

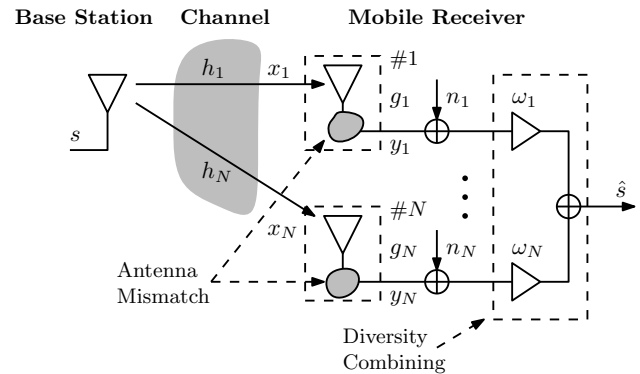


Fig. 1. System model for receive antenna diversity. The number of branches is fixed at $N = 2$.

We use an equivalent complex baseband system model as shown in Fig. 1. The system consists of a single transmit antenna at the base station and two receive antennas at the mobile terminal. The signals received from different branches are synchronized, weighted and combined before decision. The combined signal is given by

$$\hat{s} = \sum_{i=1}^2 \omega_i [g_i (h_i * s) + n_i] \quad (1)$$

where s is the complex envelope of the transmitted signal with constant transmit power, g_i and h_i are respectively the receive antenna gain and channel response at the i th branch, n_i denotes independent and identically distributed (i.i.d.) complex additive white Gaussian noise (AWGN), ω_i is the weighting coefficient applied at the i th branch before combining, and $*$ denotes convolution. For simplicity, the path loss between the transmitter and receiver is lumped into the power of the transmit signal $|s|^2$.

We assume the following conditions:

1. The channel is frequency-flat. We can therefore describe the channel between the transmit antenna and the i th receive antenna, using a complex coefficient, as

$$h_i = |h_i| e^{j\phi_i} \quad (i = 1, 2). \quad (2)$$

2. The channel consists of a large number of random paths but no line of sight (NLOS). According to the central limit theorem, both the real and imaginary parts of h_i are approximated as a Gaussian random process $\mathcal{N}(0, \sigma_i^2)$. This leads to the result that $|h_i|$ is Rayleigh distributed with

$$\mathbb{E}[|h_i|] = \sqrt{\frac{\pi}{2}} \sigma_i, \quad (3a)$$

$$\mathbb{E}[|h_i|^2] = 2\sigma_i^2. \quad (3b)$$

3. The channel is wide-sense stationary (WSS) [3], such that,

$$\mathbb{E}[|h_i|] = \text{const}, \quad (4a)$$

$$\mathbb{E}[|h_i|^2] = \text{const}. \quad (4b)$$

This condition is assumed to provide a stable communication environment for the observation of the change of system performance only due to mobile antenna mismatch, but not due to any change of the environment.

4. The channel coefficients are i.i.d., i.e., we have

$$\mathbb{E}[|h_1| |h_2|] = \mathbb{E}[|h_1|] \mathbb{E}[|h_2|], \quad (5a)$$

$$\mathbb{E}[|h_1|] = \mathbb{E}[|h_2|], \quad (5b)$$

$$\mathbb{E}[|h_1|^2] = \mathbb{E}[|h_2|^2]. \quad (5c)$$

Equation (5a) is justified by assuming that the receive antennas are sufficiently separated such that the channel and antenna correlations are negligible.

Finally, the output signal of the 1×2 SIMO (single-input and multiple-output) system described by (1) can be written as

$$\hat{s} = \sum_{i=1}^2 \omega_i (g_i |h_i| e^{j\phi_i} s + n_i). \quad (6)$$

3. User Effects on Mobile Antennas

3.1 User Effects

Both the causes and consequences of the user's impact on mobile antennas are multitudinous. On one hand, the mobile antenna performance degradation depends on multiple factors: the type of the antenna, the frequency band, the grip position, the distance from the antenna to the body (torso, shoulder or head), etc. On the other hand, the user effects are reflected in multiple aspects: the modification of radiation pattern, the reduction in radiation efficiency, the change of input impedance, detuning of the resonance frequency [9–13]. Numbers for losses due to absorption and impedance mismatch are collected from the literature and listed in Tab. 1 to help the reader develop an empirical understanding of the severity of user effects on mobile antennas.

Although the circumstances of user effects and the impact vary from case to case, the points of interest from a system perspective are clear:

1. The total amount of reduction in the effective antenna gain, which is of interest while assessing the system performance;
2. A distinction between the part of power loss due to antenna impedance mismatch and the part of power loss due to other causes, like a change in radiation pattern, and/or a reduction of the radiation efficiency.

Antenna impedance mismatch can in principle be compensated by an antenna impedance matching network [15]. Absorption can possibly be reduced or avoided, e.g., by placing the antenna in areas which are less likely to be affected

by the user's hand. However, it should also be noted that the feasibility of the latter solution is highly limited by the small size and compactness of modern mobile devices. An example of avoiding the hand effect is introduced in [13] by switching between two antennas to reduce the user-induced loss. However, in that paper, performance is only evaluated in terms of the reduction of average body loss compared to a single antenna. By applying the framework and results carried out in our paper, one can assess not only the mean performance, but also the diversity performance of such dual-antenna systems.

3.2 Antenna Model Including User Effects

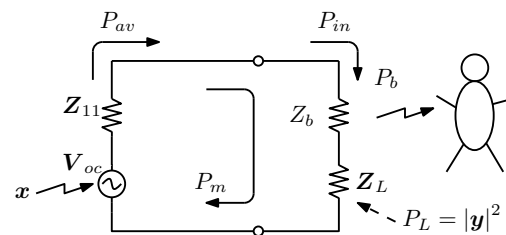


Fig. 2. Receive antenna model including user effects.

We make the following assumptions for the receive antennas:

1. The receive antennas are assumed to be isotropic (since in mobile communication we usually do not emphasize direction) and identical. We use the same model for both receive antennas. The reception of the antennas can be described by a single coefficient, the antenna gain G_i for i th antenna. (However, in the rest of this section below we drop the subscript i .)
2. The antenna separation is assumed to be large enough to allow neglecting antenna coupling. This condition, together with the independent channel condition from Section 2, guarantees uncorrelated diversity chains, and it also implies that there will be no mutual impedance between the antennas in the model.

We use an antenna model as shown in Fig. 2, which is adopted from the concept introduced in [17]. The antenna's self-impedance Z_{11} and the load impedance Z_L (the input impedance of the receiver circuit) are usually designed to be 50Ω , which means by design the load is matched to the antenna such that half of the power captured by the antenna from free space is delivered to the load. However, due to the presence of the user, the power delivery is affected via different mechanisms: 1) the user's hand modifies the radiation pattern and affects the radiation efficiency which is modeled as a gain G_r ; 2) the user's body absorbs energy P_b from the antenna; 3) the user's body introduces an equivalent series impedance Z_b , creating mismatch between the antenna and its load, and leads to the reflection of a portion (P_m) of the available power (P_{av}) back to the antenna.

Antenna	Study	Loss (dB)			Reference
		Absorption	Mismatch	Total	
Monopole	Phant. hand, simu. & meas.	—	—	5	[9]
Monopole	Human in talk position, meas.	⇒ 17, 16	2.5, 4	19.5, 20	[10]
Monopole	Phant. hand, simu.	7–8, 11	< 1	⇒ 9, 12	[11]
Monopole	Phant. hand, meas.	5.8, 5.0	0.1, 0.7	5.9, 5.7	[13]
PIFA	Phant. hand, simu. & meas.	—	—	3, 7	[9]
PIFA	Human in talk position, meas.	⇒ 13.5, 9.5	3, 2	16.5, 11.5	[10]
Nokia 6200	Human in talk position, meas.	⇒ 10, 12.5	0.5, 2.5	10.5, 15	[10]
PIFA	Phant. hand, simu.	7–8, 10.5	3	⇒ 10–11, 13.5	[11]
PIFA	Phant. hand, meas.	4.9, 6.8	4, 2	⇒ 8.9, 8.8	[12]

Note: “⇒” indicates derived numbers.

Tab. 1. Collected numbers of body loss on mobile antennas.

The available power is given by

$$P_{av} = G_o G_r |x|^2 \tag{7}$$

where x is the impinging wave, G_o is the antenna gain of an ideal antenna (without body loss) that is determined by the intrinsic characteristics of the antenna.

The power delivered to load is

$$P_L = |y|^2 = P_{av} - P_m - P_b = G_o \underbrace{\left(G_r - \frac{P_m + P_b}{G_o |x|^2} \right)}_{G_m} |x|^2 = G_o G_m |x|^2 \tag{8}$$

where y is the received signal, and G_m is a gain that is defined to account for the absorption and mismatch losses due to body and hand effects.

When the user affection is present, the gain G_m has a value between 0 and 1. Specifically, $G_m = 1$ is used to describe the ideal case that the antenna is free of user effects. We call $|10 \log G_m|$ (dB) body loss.

The phase of the whole channel, including the antenna, is estimated as a single parameter for purpose of diversity signal combining. It is therefore justified to collapse the phase of antenna into the phase of channel θ_i . We can therefore write (8) into

$$y = \sqrt{G_o G_m} x = \sqrt{G} x \tag{9}$$

where $G = G_o G_m$ is called the effective antenna gain. Considering that body loss changes at a much slower rate than fading of the channel, we model G_m , and consequently G , as a deterministic variable.

4. Figures of Merit

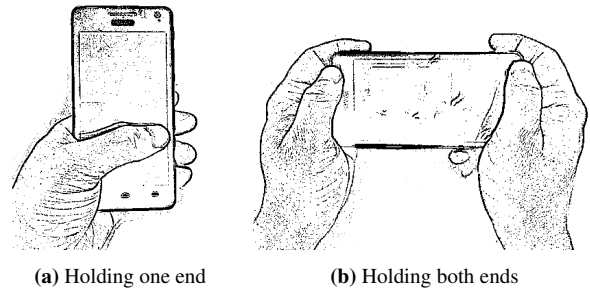


Fig. 3. Two typical grip positions of a bar phone.

In our analysis, the antenna performance degradation will be considered in two typical scenarios:

- *Body loss on a single antenna*, which describes a scenario in which only a single antenna is disturbed by the user. We can think of this situation as the user holds the lower end of a bar phone (Fig. 3(a)), which is equipped with two diversity receive antennas, one at each end. The lower antenna suffers from power loss induced by hand effects. The upper antenna, however, is not noticeably affected and thus is considered ideal.
- *Equal body loss on both antennas*, which describes another scenario in which both antennas are almost equally influenced. It would be such a case when the user holds both ends of the phone (Fig. 3(b)).

The system performance will be evaluated with respect to the following measures:

- *Array gain*, which is the increase of the mean SNR of the combined signal relative to the mean SNR of an ideal single-input single-output (SISO) link. Array gain is shown as a shift of the bit error rate (BER) curve towards lower SNR [18],[19, p. 8].

- *Diversity gain*, which is the gain reflected in the BER plot as a further shift (due to a change of the slope) of the curve (on top of array gain) towards lower SNR² [18].

- *BER performance*, which we give as the average error probability of uncoded BPSK:

$$P_e = \int_0^\infty Q(\sqrt{2\gamma_b}) p(\gamma_b) d\gamma_b \quad (10)$$

where γ_b (or E_b/N_0) is SNR per bit, and $Q(\sqrt{2\gamma_b})$ is the error probability function of uncoded BPSK in AWGN channels [21, p. 256]. Note that the BER depends on γ_b , which is related to γ by the spectral efficiency ρ (bit/s/Hz) as: $\gamma_b = \gamma/\rho$. The expression for $p(\gamma_b)$ is given in Appendix A.

- *Diversity order*, which is the negative of the asymptotic slope of the average BER curve $P_e(\text{SNR})$ with respect to SNR in a log-log plot [1],[22, pp. 145–146], i.e.,

$$d = - \lim_{\text{SNR} \rightarrow \infty} \frac{\log P_e(\text{SNR})}{\log \text{SNR}}. \quad (11)$$

- *Ergodic capacity*, which is the Shannon capacity calculated in an average sense in the context of Rayleigh fading [1, 23, 24], is expressed in bps/Hz and given as

$$C = \int_0^\infty \log_2(1 + \gamma) p(\gamma) d\gamma. \quad (12)$$

As clarified by Günther in [24], the reader should note that although (10) and (12) look quite similar in form, they apply to rather different situations. Equation (10) holds for a constant rate transmission over a fading and noisy channel and describes the probability of error. Equation (12) applies to the case where the coding (and correspondingly the rate) is adapted to achieve error-free transmission at the Shannon limit [25] and gives the average capacity of such a transmission scheme.

5. Diversity Combining

5.1 Maximal Ratio Combining

Maximal ratio combining is the optimal combining method that gives the maximum combined SNR. MRC uses weighting coefficients which, according to [3, p. 313], are

$$\omega_i = \frac{y_i^*}{\sigma_{n_i}^2} \quad (i = 1, 2) \quad (13)$$

where $\sigma_{n_i}^2 = \sigma_n^2$ denotes the variance of noise n_i .

The SNR of the MRC-combined signal is

$$\gamma = \frac{\left| \sum_{i=1}^2 \omega_i y_i \right|^2}{\sum_{i=1}^2 |\omega_i|^2 \sigma_{n_i}^2} = \gamma_1 + \gamma_2 \quad (14)$$

where $\gamma_i = |y_i|^2 / \sigma_n^2$ ($i = 1, 2$) is the SNR of the signal received at the i th branch.

In order to study the performance in terms of body loss, we define

$$\gamma_{oi} = \frac{G_{oi} |x_i|^2}{\sigma_n^2} = G_{oi} \gamma_{xi} \quad (15)$$

which is essentially a hypothetical SNR that would be obtained at the i th branch if there were no body loss at the antenna. Using the condition that the channel coefficients h_i ($i = 1, 2$) are i.i.d., we further define $\bar{\gamma}_o$, which represents the mean SNR of the signal received by an ideal antenna (without body loss), as

$$\bar{\gamma}_o = \bar{\gamma}_{oi} = \frac{G_{oi}}{\sigma_{n_i}^2} \mathbb{E} \left[|x_i|^2 \right] \quad (i = 1, 2). \quad (16)$$

Because of (9), we have

$$\gamma_i = G_{mi} \gamma_{oi}, \quad (17a)$$

$$\bar{\gamma}_i = G_{mi} \bar{\gamma}_o. \quad (17b)$$

By taking the expectation of (14) and using (17), we obtain the mean output SNR of the MRC-combined signal in terms of body loss:

$$\bar{\gamma} = \bar{\gamma}_o (G_{m1} + G_{m2}). \quad (18)$$

The PDF of γ_i is (see Appendix A)

$$p_{\gamma_i}(\gamma_i) = \frac{1}{\bar{\gamma}_i} \exp\left(-\frac{\gamma_i}{\bar{\gamma}_i}\right). \quad (19)$$

The Cumulative Distribution Function (CDF) of γ , which gives the outage SNR performance, can be calculated from

$$P_\gamma(\gamma) = \int_0^\gamma \int_0^{\gamma-\gamma_2} p_{\gamma_1}(\gamma_1) p_{\gamma_2}(\gamma_2) d\gamma_1 d\gamma_2. \quad (20)$$

Equation (20) produces conditional results for $\gamma_1 \neq \gamma_2$ and $\gamma_1 = \gamma_2$.

1. For $\gamma_1 \neq \gamma_2$, (20) gives

$$P_\gamma(\gamma) = 1 - \frac{\bar{\gamma}_1}{\bar{\gamma}_1 - \bar{\gamma}_2} \exp\left(-\frac{\gamma}{\bar{\gamma}_1}\right) + \frac{\bar{\gamma}_2}{\bar{\gamma}_1 - \bar{\gamma}_2} \exp\left(-\frac{\gamma}{\bar{\gamma}_2}\right) \quad (21)$$

which can be written in terms of body loss as

$$P_\gamma(\gamma) = 1 - \frac{G_{m1}}{G_{m1} - G_{m2}} \exp\left(-\frac{\gamma}{\bar{\gamma}_1}\right) + \frac{G_{m2}}{G_{m1} - G_{m2}} \exp\left(-\frac{\gamma}{\bar{\gamma}_2}\right). \quad (22)$$

The PDF of γ can be readily calculated from

²There is no unique definition of *diversity gain*. It has also been defined in the log-log plot as the negative slope of the average BER versus SNR [19, p. 8] or as the negative slope of the average BER versus SNR at infinite SNR [20, p. 70]. The latter is actually what we define as *diversity order* in this article.

$$p_\gamma(\gamma) = \frac{d}{d\gamma} P_\gamma(\gamma). \quad (23)$$

The average bit error probability of BPSK in Rayleigh fading channels using MRC combining can be calculated as (see Appendix B)

$$P_e = \int_0^\infty Q(\sqrt{2\gamma_b}) p(\gamma_b) d\gamma_b \quad (24a)$$

$$= \frac{1}{2} \left(1 - \frac{G_{m1}}{G_{m1} - G_{m2}} \sqrt{\frac{G_{m1} \bar{\gamma}_{bo}}{1 + G_{m1} \bar{\gamma}_{bo}}} + \frac{G_{m2}}{G_{m1} - G_{m2}} \sqrt{\frac{G_{m2} \bar{\gamma}_{bo}}{1 + G_{m2} \bar{\gamma}_{bo}}} \right). \quad (24b)$$

- For $\gamma_1 = \gamma_2$, follow the same procedure as above resulting in

$$P_\gamma(\gamma) = 1 - \left(1 + \frac{\gamma}{G_{m1} \bar{\gamma}_o} \right) \exp\left(-\frac{\gamma}{G_{m1} \bar{\gamma}_o}\right). \quad (25)$$

The average bit error probability for uncoded BPSK is

$$P_e = \frac{1}{2} \left[1 - \left(\frac{G_{m1} \bar{\gamma}_{bo}}{1 + G_{m1} \bar{\gamma}_{bo}} \right)^{\frac{3}{2}} \left(1 + \frac{3}{2} \frac{1}{G_{m1} \bar{\gamma}_{bo}} \right) \right]. \quad (26)$$

5.2 Equal Gain Combining

With balanced branches, EGC is a sub-optimal but attractive solution because it does not require estimation of the fading amplitudes and thus is easier to implement compared to MRC [3, 4]. However, as we will show later, when diversity branches are not balanced to certain extent, EGC may perform worst among the three combining methods we are discussing.

The EGC method uses the weighting coefficients as defined by [3, p. 313]

$$\omega_i = \exp(-\theta_i) \quad (27)$$

where θ_i is the phase of channel h_i .

The SNR of the EGC-combined signal is

$$\gamma = \frac{\left| \sum_{i=1}^2 \omega_i y_i \right|^2}{\sum_{i=1}^2 |\omega_i|^2 \sigma_n^2} = \frac{1}{2\sigma_n^2} (|y_1| + |y_2|)^2. \quad (28)$$

By taking the expectation of (28) (see Appendix C), we obtain the mean output SNR of the EGC-combined signal which is

$$\bar{\gamma} = \frac{1}{2} \left(\sum_{i=1}^2 G_{mi} + \frac{\pi}{4} \sum_{i,j=1(i \neq j)}^2 \sqrt{G_{mi} G_{mj}} \right) \bar{\gamma}_o. \quad (29)$$

The CDF of γ is given in (30) (see Appendix D).

With EGC combining, the average bit error probability for uncoded BPSK in Rayleigh fading channels is calculated using (24a) and given in (31).

5.3 Selection Combining

Selection combining is a scheme that instantaneously selects the branch with the highest SNR, i.e.,

$$\omega_i = \begin{cases} 1 & \text{if } i = \arg \max_i \gamma_i, \\ 0 & \text{otherwise.} \end{cases} \quad (32)$$

The probability of the SNR at the i th branch being less than or equal to some value γ is given in [3, p. 311] as

$$\Pr(\gamma_i \leq \gamma) = 1 - \exp\left(-\frac{\gamma}{\bar{\gamma}_i}\right). \quad (33)$$

The probability that the SNRs at all branches are simultaneously less than or equal to γ is

$$P_\gamma(\gamma) = \Pr(\gamma_1, \gamma_2 \leq \gamma) = \prod_{i=1}^2 \Pr(\gamma_i \leq \gamma) = \prod_{i=1}^2 \left[1 - \exp\left(-\frac{\gamma}{G_{mi} \bar{\gamma}_o}\right) \right]. \quad (34)$$

$$P_\gamma(\gamma) = 1 - \frac{G_{m1}}{G_{m1} + G_{m2}} \exp\left(-\frac{2\gamma}{G_{m1} \bar{\gamma}_o}\right) - \frac{G_{m2}}{G_{m1} + G_{m2}} \exp\left(-\frac{2\gamma}{G_{m2} \bar{\gamma}_o}\right) - \frac{1}{G_{m1} + G_{m2}} \sqrt{2\pi} \frac{G_{m1} G_{m2}}{G_{m1} + G_{m2}} \frac{\gamma}{\bar{\gamma}_o} \cdot \exp\left(-\frac{2\gamma}{G_{m1} + G_{m2}} \frac{\gamma}{\bar{\gamma}_o}\right) \left(\operatorname{erf}\left(\sqrt{\frac{2}{G_{m1} + G_{m2}} \frac{G_{m1}}{G_{m2}} \frac{\gamma}{\bar{\gamma}_o}}\right) + \operatorname{erf}\left(\sqrt{\frac{2}{G_{m1} + G_{m2}} \frac{G_{m2}}{G_{m1}} \frac{\gamma}{\bar{\gamma}_o}}\right) \right) \quad (30)$$

$$P_e = \frac{1}{2} \left[1 - \frac{G_{m1}}{G_{m1} + G_{m2}} \sqrt{\frac{G_{m1} \bar{\gamma}_{bo}}{2 + G_{m1} \bar{\gamma}_{bo}}} - \frac{G_{m2}}{G_{m1} + G_{m2}} \sqrt{\frac{G_{m2} \bar{\gamma}_{bo}}{2 + G_{m2} \bar{\gamma}_{bo}}} - \sqrt{2} \frac{G_{m1} G_{m2}}{G_{m1} + G_{m2}} \frac{1}{\bar{\gamma}_{bo}} \frac{\bar{\gamma}_{bo}}{2 + (G_{m1} + G_{m2}) \bar{\gamma}_{bo}} \cdot \left(\sqrt{\frac{G_{m1}}{G_{m1} + G_{m2} + \frac{1}{2} G_{m2} (G_{m1} + G_{m2}) \bar{\gamma}_{bo}}} + \sqrt{\frac{G_{m2}}{G_{m1} + G_{m2} + \frac{1}{2} G_{m1} (G_{m1} + G_{m2}) \bar{\gamma}_{bo}}} \right) \right] \quad (31)$$

Using (23) and the method of integration by parts, we can compute the mean SNR of the SC-combined signal as

$$\begin{aligned} \bar{\gamma} &= \int_0^\infty \gamma p_\gamma(\gamma) d\gamma \\ &= \left(G_{m1} + G_{m2} - \frac{G_{m1}G_{m2}}{G_{m1} + G_{m2}} \right) \bar{\gamma}_o. \end{aligned} \quad (35)$$

The bit error probability for uncoded BPSK in Rayleigh fading channels using SC combining is calculated using (24a), which gives

$$P_e = \frac{1}{2} \left(1 - \sqrt{\frac{G_{m1}\bar{\gamma}_o}{G_{m1}\bar{\gamma}_o + 1}} - \sqrt{\frac{G_{m2}\bar{\gamma}_o}{G_{m2}\bar{\gamma}_o + 1}} + \sqrt{\frac{G_{12}\bar{\gamma}_o}{G_{12}\bar{\gamma}_o + 1}} \right) \quad (36)$$

where $G_{12} = G_{m1}G_{m2}/(G_{m1} + G_{m2})$.

6. Performance Analysis

6.1 Array Gain

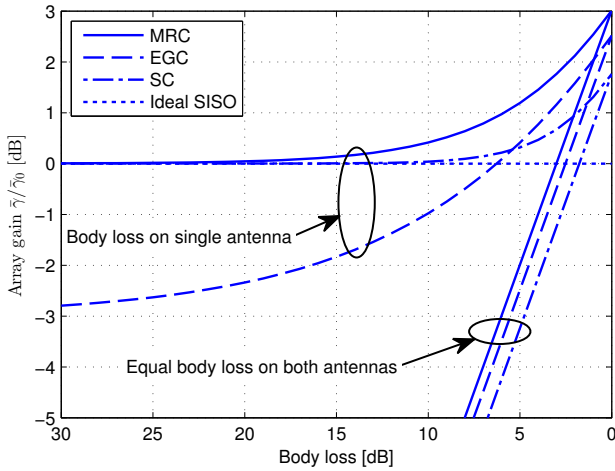


Fig. 4. Array gains of different diversity combining methods versus body loss. In case of “equal body loss on both antennas”, body loss is per antenna.

The array gain, by definition, is calculated as $\bar{\gamma}/\bar{\gamma}_o$. The array gains of MRC, EGC, and SC with two receive antennas are found, respectively, from (18), (29) and (35). The results of body loss on a single antenna and equal body loss on both antennas are plotted in Fig. 4.

In case of body loss on a single antenna, when body loss rises up to a certain level, MRC and SC lose their array gains and end up having the same mean SNR as in the ideal SISO case. Interestingly, we also see that when the body loss is larger than about 5.5 dB, the array gain of EGC is even worse than that of SC, and finally ends up at -3 dB. This phenomenon can be interpreted like this: in case of

a very high body loss on a single antenna, the signal power received from that branch is relatively small. The EGC combining method only obtains negligible signal power from that branch, but brings in the noise without attenuation, i.e., there is 3 dB more noise but nearly no gain in signal power. As a result, there is 3 dB reduction in average SNR compared to an ideal single branch.

The case of equal body loss on both antennas is essentially equivalent to a reduction in the transmit power in an ideal system. The mean SNRs for all combining methods drop linearly with the level of body loss per antenna.

After all, we conclude that body loss on a single antenna has limited (bounded) impact on the mean combined SNR, but equal body loss on both antennas results in an unlimited (unbounded) reduction of the mean combined SNR.

6.2 Distribution of the Combined SNR

The distribution of the combined SNR is analyzed using the Complementary Cumulative Distribution Function (CCDF), which is a measure of the reliability of the communication link. The CCDF of the combined SNR for all three combining methods are plotted in Fig. 5 using (22), (25), (30), and (34).

In the region where the reliability is larger than 90%, the relative SNR lines are (asymptotically) becoming straight. Body loss of G_m dB on single antenna tends to reduce the combined SNR (at same reliability level) by half of G_m dB. It is important to note that the reduction for MRC and SC is bounded by the SNR of ideal SISO, and for EGC it is bounded by a value of 3 dB below the SNR of ideal SISO. This is seen in Fig. 5(a). For example, at 99% reliability, a body loss of 7 dB and 14 dB on single antenna reduces the combined SNR of all three combining techniques, respectively, by 3.5 dB and 7 dB.

Since equal body loss of G_m dB on both antennas can be viewed equivalently as a reduction in transmit power by G_m dB, the impact of such a body loss scenario corresponds to a shift of the SNR curves as shown in Fig. 5(b). Body loss of G_m dB on both antennas causes a decrease of combined SNR by an amount that equals to G_m dB. This is in contrast to the case of body loss on a single antenna, in which the reduction of SNR is bounded.

MRC in all cases outperforms EGC and SC. Except for the bounded region (upper right) in Fig. 5(a) the combined SNR of EGC and SC is, respectively, about 0.5 dB and 1.5 dB less than the SNR of MRC.

6.3 BER Performance

The BER curves for uncoded BPSK with different combining methods are plotted in Fig. 6 using (24b), (26), (31) and (36). The theoretical results agree with the simulated results that we presented in [26].

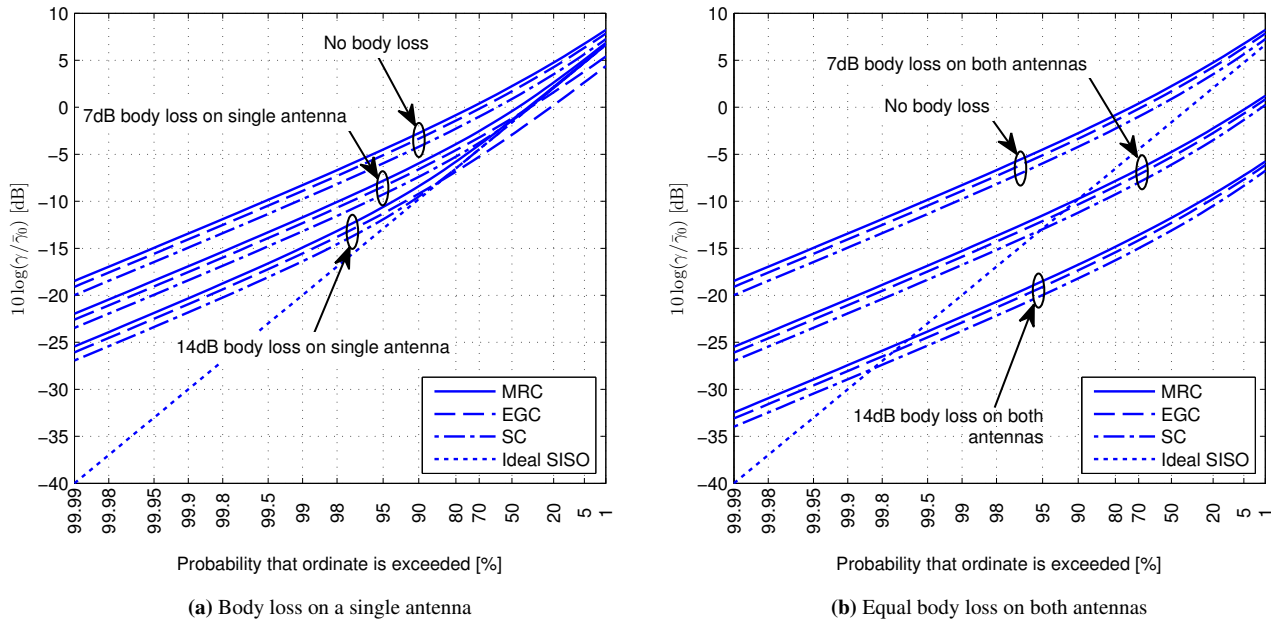


Fig. 5. The ccdf function of the combined SNR for different diversity combining methods versus body loss.

The BER with body loss on a single antenna is plotted in Fig. 6(a). First, we define high SNR regime and low SNR regime depending on if E_b/N_0 exceeds the level of body loss or not. That is, in case of 7 dB body loss, the division is 7 dB in terms of E_b/N_0 , and in case of 14 dB body loss, the division is 14 dB in terms of E_b/N_0 . In the low SNR regime, body loss tends to flatten the BER curves towards the performance of ideal SISO. EGC exhibits an even worse BER performance than ideal SISO. However, the impact in the high SNR regime is limited and all diversity methods show remarkable gain over ideal SISO. 7 dB body loss on a single antenna shifts the BER curves to the right by about 3.5 dB, and 14 dB body loss on a single antenna shifts the BER curve to the right by about 7 dB. In the high SNR regime the slope doesn't seem to be notably changed and these diversity schemes still show remarkable improvements. It is important to recognize that the power loss due to body loss on a single antenna is bounded. The BER performance of MRC and SC is never below that of ideal SISO. However, EGC can show at maximum 3 dB power loss with respect to ideal SISO.

In contrast to the impact of body loss on a single antenna, body loss on both antennas has twice as much of power loss. Moreover, the power loss in this case is not bounded. As can be seen in Fig. 6(b), at high SNR, 7 dB body loss on both antennas shift the BER curves to the right by about 7 dB, and 14 dB body loss on both antennas shift the BER curves to the right by about 14 dB. At high SNR, the curve slopes are close to that of ideal systems in an asymptotic manner.

6.4 Diversity Order

The negative slopes of the BER curves of Fig. 6 are calculated numerically and plotted in Fig. 7. We see that the change of slope due to body loss happens in the low SNR regime. As SNR increases, the slope tends asymptotically to 2, which means the bit error rate is decreasing proportional to γ^{-2} . According to the definition of *diversity order* given in Section 4, the diversity order for all the combining methods in any body loss scenario is still 2, i.e., body loss does not change the diversity order.

The definition of diversity order at *infinite SNR* has its limitation. As reflected in our examples, it may not reflect the diversity performance of a system in practical SNR ranges.

6.5 Ergodic Capacity

As shown in Fig. 8, where we plot the ergodic capacity against $10 \log(\bar{\gamma}_o)$, it is immediately apparent that at high SNR, ergodic capacities of both SISO and diversity systems have the same slope and increase linearly with $10 \log(\bar{\gamma}_o)$. The slope can be found numerically as

$$\lim_{\bar{\gamma}_o \rightarrow \infty} \frac{\int_0^\infty \log_2(1 + \gamma) \frac{1}{\bar{\gamma}_o} \exp\left(-\frac{\gamma}{\bar{\gamma}_o}\right) d\gamma}{10 \log \bar{\gamma}_o} = \frac{1}{10} \log_2(10) = 0.332 \text{ bps/Hz/dB}. \quad (37)$$

Equation (37) indicates an increase of 0.332 bps/Hz in capacity per decibel increase in $\bar{\gamma}_o$.

³Fig. 9 facilitates the calculation: at $\bar{\gamma}_o = 30$ dB with 0 dB body loss, the difference between the MRC capacity and ideal SISO capacity is $10.58 - 9.14 = 1.44$ bps/Hz, which translates into a power gain of $1.44/0.332 = 4.34$ dB.

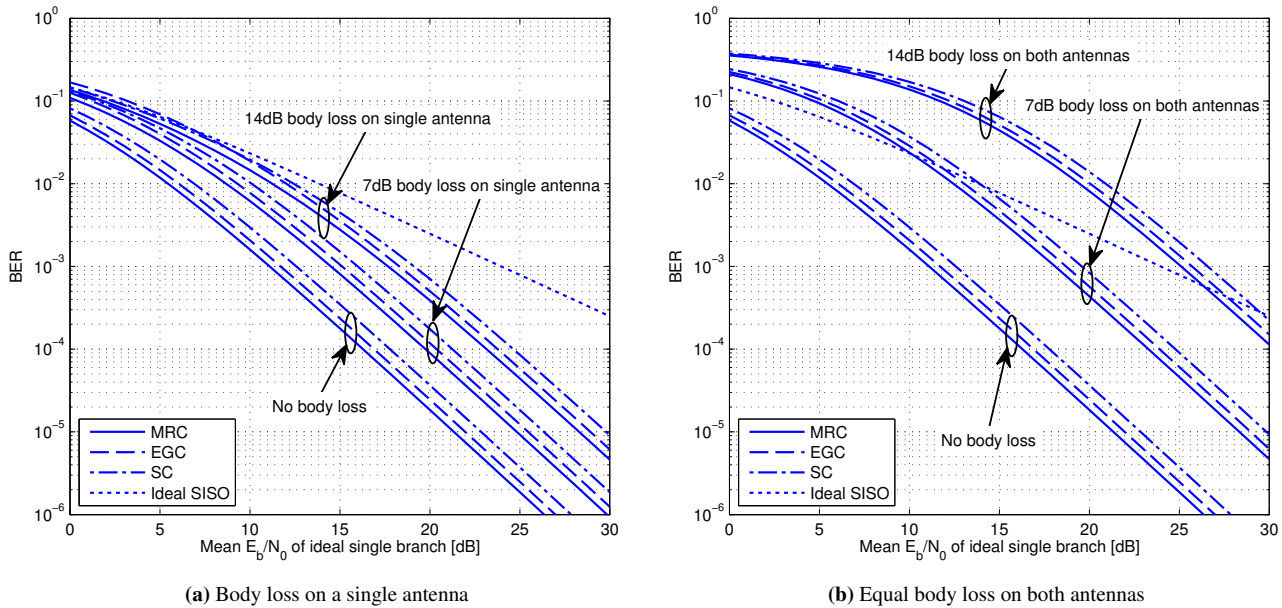


Fig. 6. BER performance using uncoded BPSK.

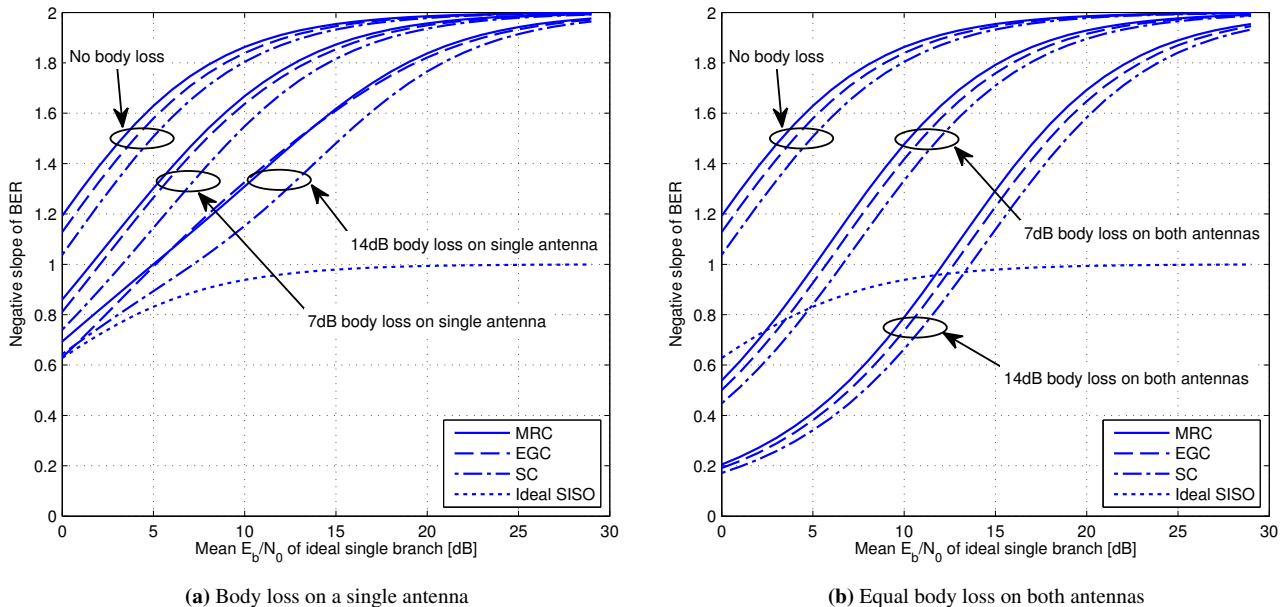
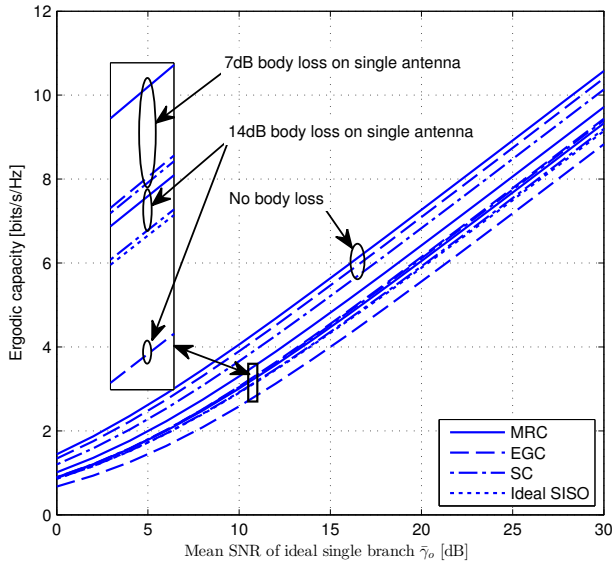


Fig. 7. Negative slopes of the BER curves in Fig. 6.

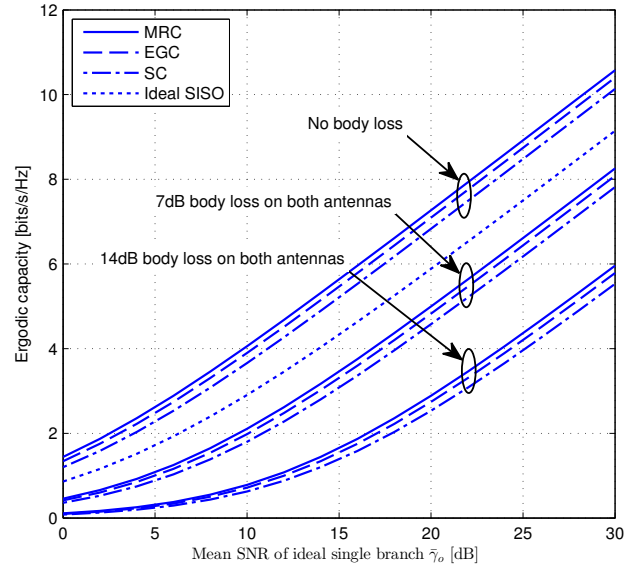
Comparing the capacities of three combining methods, MRC outperforms EGC and SC in all cases. At high SNR in the ideal case (no body loss), MRC has an advantage of 1.44 bps/Hz³ over ideal SISO, which means a power gain of 4.34 dB with regard to ideal SISO. One may also notice in Fig. 8(a) that, in case of no body loss or 7 dB body loss on a single antenna, EGC has a larger capacity than SC, but in case of 14 dB body loss on a single antenna, EGC has lower performance than SC. This phenomenon can be easier observed in Fig. 9, which depicts the reduction of capacity due to body loss on a single antenna with $\bar{\gamma}_0$ being fixed at 30 dB. When single antenna body loss rises, the capacities of MRC and SC drop down asymptotically to the same capacity as ideal SISO. However, EGC ends up with a capacity that is 1 bps/Hz below that of ideal SISO, corresponding to a drop

of SNR by $1/0.332 = 3$ dB. Assuming branch 2 is the one with body loss and branch 1 is ideal, the phenomenon can be explained as follows:

1. MRC scales the signal and noise at each branch before combining and leads to $\gamma = \gamma_1 + \gamma_2 \geq \gamma_1$ (see (14)), which implies that the MRC won't give an SNR worse than ideal SISO.
2. The SC method instantaneously selects the branch of higher SNR, and so there is $\gamma = \max(\gamma_1, \gamma_2) \geq \gamma_1$. Again the combined SNR cannot be worse than that of ideal SISO.



(a) Body loss on a single antenna



(b) Equal body loss on both antennas

Fig. 8. Ergodic capacity.

3. From (28), we know that when $|y_2| < |y_1| \cdot (\sqrt{5} - 1)/2$, EGC can result in a combined SNR below that of ideal SISO. When branch 2 is heavily attenuated, e.g., above 10 dB in Fig. 9, the probability of such negative impact can be large enough such that the mean capacity is lower than ideal SISO. For very large body loss, only a copy of unattenuated noise but negligibly small signal are added in. This leads to 3 dB reduction of the combined SNR.

Finally, we conclude that body loss on a single antenna has limited impact on ergodic capacity whereas body loss on both antennas can have very large impact and cause significant reduction in ergodic capacity. For MRC and SC, body loss on a single antenna to whatever degree does not cause a capacity reduction more than 1.44 bps/Hz (or 4.34 dB in power loss). For EGC the reduction in capacity is a bit larger, which is 1.57 bps/Hz (or 4.73 dB in power loss) in case of 14 dB body loss on a single antenna and 2.224 bps/Hz (or 6.70 dB in power loss) for infinite body loss. In contrast, equal body loss on both antennas, which can be viewed, equivalently, as a reduction in transmit power, leads to a capacity loss proportional to the level of body loss, that is, $0.332 \times |10 \log G_m|$ bps/Hz ($G_m = G_{mi}$, $i = 1, 2$). This is reflected in Fig. 8(b), where we see 7 dB and 14 dB body loss on both antennas cause, respectively, a reduction of ergodic capacity by 2.33 bps/Hz (or 7 dB in power loss) and 4.65 bps/Hz (or 14 dB in power loss).

7. Conclusion

Out of the comparative study of the impact of body loss on the performances of MRC, EGC and SC, we can make the

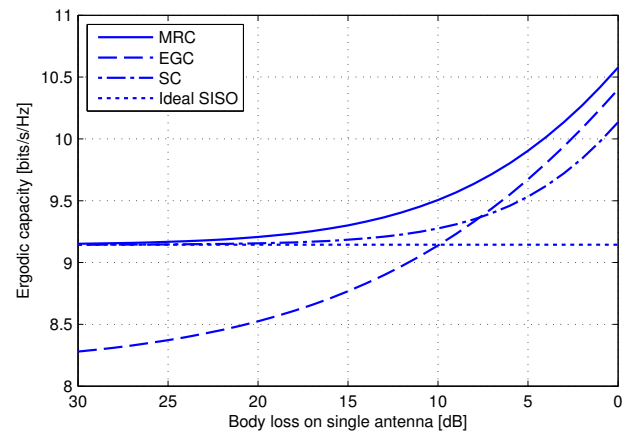


Fig. 9. Ergodic capacity versus body loss on a single antenna ($\bar{\gamma}_o = 30$ dB).

following conclusions:

- The reduction of the combined SNR due to body loss on a single antenna is bounded. The bound for the combined SNR of MRC and SC is the SNR of ideal SISO, and the bound for EGC is 3 dB below the SNR of ideal SISO. In the region where the performance curve is straight and showing 2nd order diversity in the distribution plot (Fig. 5(a)), the BER plot (Fig. 6(a)) and the ergodic capacity plot (Fig. 8(a)), the impact of G_m dB body loss on a single antenna is reflected as half G_m dB power loss but within the bound.
- The reduction of the combined SNR due to equal body loss on both antennas is not bounded. G_m dB body loss on both antennas, which is equivalent to a reduction of the transmit power by G_m dB, leads to a reduction of the combined SNR also by G_m dB. Such a G_m dB

power loss shows up in the distribution plot (Fig. 5(b)), the BER plot (Fig. 6(b)) and the ergodic capacity plot (Fig. 8(b)).

- Body loss on a single antenna does not change the diversity order but does reduce the slope of BER curve in the low SNR region. This results in degradation of the BER performance.
- The level of body loss on a single antenna, above which EGC loses advantage over SC, is 5.5 dB in the mean SNR plot (Fig. 4) and 8 dB in the ergodic capacity plot (Fig. 9).
- At 90% reliability, the diversity system with 14 dB body loss on a single antenna or 7 dB body loss on both antennas can only support the same level of minimum output SNR as ideal SISO (Fig. 5).
- In the range of 10–15 dB in terms of ideal single branch SNR (denoted by $\bar{\gamma}_o$), 14 dB body loss on single antenna causes the diversity system to show only a small gain compared to ideal SISO, and 7 dB body loss on both antennas causes the diversity system to lose power gain compared to ideal SISO (Fig. 6).
- Finally, 1–4 dB body loss on single antenna, which introduces only 0.5–2 dB reduction of the combined SNR, generally does not have significant impact in a diversity system with uncorrelated branches.

Appendix A. Rayleigh Distribution

Since signal y_i is received from the Rayleigh fading channel, the PDF of $|y_i|$ is

$$p(|y_i|) = \frac{|y_i|}{\Omega_i} \exp\left(-\frac{|y_i|^2}{2\Omega_i}\right)$$

where $\Omega_i = \frac{1}{2}\mathbb{E}[|y_i|^2]$. Define the SNR at the i th branch as $\gamma_i = \text{Signal power}/\text{Mean noise power} = |y_i|^2/\sigma_{n_i}^2$. And then the corresponding mean SNR is

$$\bar{\gamma}_i = \frac{2\Omega_i}{\sigma_{n_i}^2} = \frac{2\Omega_i}{\sigma_n^2}.$$

The PDF of γ_i can be calculated via probability transformation:

$$p(\gamma_i) = \frac{p(|y_i|)}{d\gamma_i/d|y_i|} = \frac{1}{\bar{\gamma}_i} \exp\left(-\frac{\gamma_i}{\bar{\gamma}_i}\right). \quad (38)$$

Suppose BPSK (with certain pulse shaping) achieves a transmission rate of R bps in a B Hz wide single-sided spectrum in baseband. The spectrum efficiency of the communication is $\rho = R/B$ bps/Hz. Let N_0 be the single-sided noise power spectral density, then the SNR per bit, γ_{bi} is

$$\gamma_{bi} = (E_b/N_0)_i = \frac{\gamma_i}{\rho}.$$

Again using distribution transformation (as in (38)), we have

$$p(\gamma_{bi}) = \frac{p(\gamma_i)}{d\gamma_{bi}/d\gamma_i} = \frac{1}{\bar{\gamma}_{bi}} \exp\left(-\frac{\gamma_{bi}}{\bar{\gamma}_{bi}}\right). \quad (39)$$

Similar to $\bar{\gamma}_o$, we correspondingly define the mean SNR per bit for ideal SISO communication, $\bar{\gamma}_{bo}$ as

$$\bar{\gamma}_{bo} = \frac{\bar{\gamma}_o}{\rho}.$$

And also similar to (17), there are

$$\gamma_{bi} = G_{mi}\gamma_{bo}, \quad \bar{\gamma}_{bi} = G_{mi}\bar{\gamma}_{bo}.$$

Appendix B. BER Calculation

We demonstrate the calculation of (24a), which is the BER for MRC combining under condition $\bar{\gamma}_1 = \bar{\gamma}_2$. The same procedure also applies to other BER calculations involved in this paper.

The calculation of (24a) is started by first transforming the Q function into the erfc function:

$$\begin{aligned} Q(x) \Big|_{x=\sqrt{2\gamma_b}} &= \frac{1}{2} \operatorname{erfc}\left(\frac{x}{\sqrt{2}}\right) \Big|_{x=\sqrt{2\gamma_b}} \\ &= \frac{1}{2} \frac{2}{\sqrt{\pi}} \int_x^\infty e^{-t^2} dt \Big|_{x=\sqrt{2\gamma_b}} \\ &= \frac{1}{\sqrt{\pi}} \int_{\sqrt{\gamma_b}}^\infty \exp(-t^2) dt. \end{aligned}$$

Hence,

$$\begin{aligned} P_e &= \int_0^\infty Q(\sqrt{2\gamma_b}) p(\gamma_b) d\gamma_b \\ &= \frac{1}{\sqrt{\pi}} \int_0^\infty \int_{\sqrt{\gamma_b}}^\infty \exp(-t^2) \frac{1}{\bar{\gamma}_{b1} - \bar{\gamma}_{b2}} \\ &\quad \cdot \left(\exp\left(-\frac{\gamma_b}{\bar{\gamma}_{b1}}\right) - \exp\left(-\frac{\gamma_b}{\bar{\gamma}_{b2}}\right) \right) dt d\gamma_b. \quad (40) \end{aligned}$$

An exchange of order of integration is necessary to make further calculations of the two dimensional integral in (40) possible. The area of integration is plotted in Fig. 10 (the shaded area), to help us come up with

$$\int_0^\infty \int_{\sqrt{\gamma_b}}^\infty dt d\gamma_b = \int_0^\infty \int_0^{t^2} d\gamma_b dt.$$

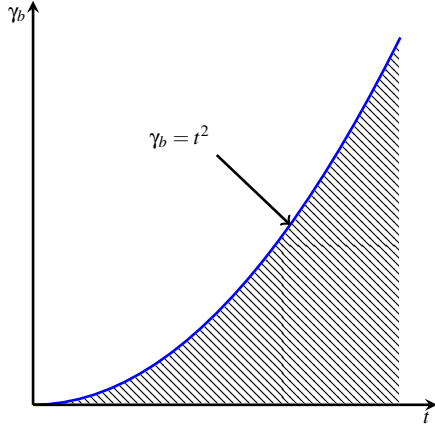


Fig. 10. The area of integration of the two dimensional integral in (40).

Now, (40) can be written into

$$\begin{aligned} P_e &= \frac{1}{\sqrt{\pi}} \int_0^\infty \int_0^{t^2} \exp(-t^2) \frac{1}{\bar{\gamma}_{b1} - \bar{\gamma}_{b2}} \\ &\quad \cdot \left(\exp\left(-\frac{\gamma_b}{\bar{\gamma}_{b1}}\right) - \exp\left(-\frac{\gamma_b}{\bar{\gamma}_{b2}}\right) \right) d\gamma_b dt \\ &= \frac{1}{\sqrt{\pi}} \int_0^\infty \exp(-t^2) \left(1 - \frac{\bar{\gamma}_{b1}}{\bar{\gamma}_{b1} - \bar{\gamma}_{b2}} \exp\left(-\frac{t^2}{\bar{\gamma}_{b1}}\right) \right. \\ &\quad \left. + \frac{\bar{\gamma}_{b2}}{\bar{\gamma}_{b1} - \bar{\gamma}_{b2}} \exp\left(-\frac{t^2}{\bar{\gamma}_{b2}}\right) \right) dt. \end{aligned}$$

By using

$$\int_0^\infty \exp(-(1+\alpha)t^2) dt = \frac{\sqrt{\pi}}{2} \frac{1}{\sqrt{1+\alpha}}$$

we find

$$\begin{aligned} P_e &= \frac{1}{2} \left(1 - \frac{\bar{\gamma}_{b1}}{\bar{\gamma}_{b1} - \bar{\gamma}_{b2}} \sqrt{\frac{\bar{\gamma}_{b1}}{1 + \bar{\gamma}_{b1}}} \right. \\ &\quad \left. + \frac{\bar{\gamma}_{b2}}{\bar{\gamma}_{b1} - \bar{\gamma}_{b2}} \sqrt{\frac{\bar{\gamma}_{b2}}{1 + \bar{\gamma}_{b2}}} \right) \\ &= \frac{1}{2} \left(1 - \frac{G_{m1}}{G_{m1} - G_{m2}} \sqrt{\frac{G_{m1} \bar{\gamma}_{bo}}{1 + G_{m1} \bar{\gamma}_{bo}}} \right. \\ &\quad \left. + \frac{G_{m2}}{G_{m1} - G_{m2}} \sqrt{\frac{G_{m2} \bar{\gamma}_{bo}}{1 + G_{m2} \bar{\gamma}_{bo}}} \right). \end{aligned}$$

Appendix C. Mean SNR of EGC

Taking the expectation of (28) yields

$$\begin{aligned} \bar{\gamma} &= \frac{1}{N\sigma_n^2} \mathbb{E} [(|y_1| + |y_2|)^2] \\ &= \frac{1}{N\sigma_n^2} \mathbb{E} \left[\left[\sum_{i=1}^2 g_{mi} g_{oi} |x_i| \right]^2 \right] \\ &= \frac{1}{N\sigma_n^2} \mathbb{E} \left[\sum_{i,j=1}^2 g_{mi} g_{oi} |x_i| g_{mj} g_{oj} |x_j| \right] \\ &= \frac{1}{N\sigma_n^2} \sum_{i,j=1}^2 g_{mi} g_{oi} g_{mj} g_{oj} \mathbb{E} [|x_i| |x_j|]. \end{aligned} \quad (41)$$

In case of $i \neq j$ in (41), we apply the i.i.d. condition of the channel h_i introduced in Section 2, which leads to

$$\begin{aligned} \mathbb{E} [|x_i| |x_j|] &= \mathbb{E} [|x_i|] \mathbb{E} [|x_j|] \quad (i \neq j) \\ &= \frac{\pi}{2} \sigma_i^2 = \frac{\pi}{2} \sigma_j^2. \end{aligned}$$

Recall the definition in (16), and then we can write (41) into

$$\bar{\gamma} = \frac{1}{2} \left(\sum_{i=1}^2 G_{mi} + \frac{\pi}{4} \sum_{i,j=1(i \neq j)}^2 \sqrt{G_{mi} G_{mj}} \right) \bar{\gamma}_o. \quad (42)$$

Appendix D. CDF of EGC

In this section, we calculate the cdf of the SNR of the EGC-combined signal (28). Mathematically, we should recognize that it is about to find the distribution of a function of two random variables, namely, $|y_1|$ and $|y_2|$.

The CDF of $|y|$ can be computed from

$$\begin{aligned} P(|y|) &= \Pr(|y_1| + |y_2| \leq |y|) \\ &= \int \int_{|y_1|, |y_2| \in \mathbb{D}} p(|y_1|, |y_2|) d|y_1| d|y_2| \end{aligned} \quad (43)$$

where $p(|y_1|, |y_2|)$ is the joint distribution of $|y_1|$ and $|y_2|$, and \mathbb{D} is the shaded area depicted in Fig. 11 which is defined by $|y_1| + |y_2| \leq |y|$.

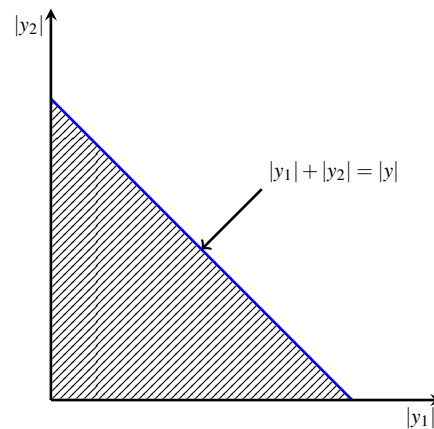


Fig. 11. The area of integration of the two dimensional integral in (43).

Since y_1 and y_2 are independent,

$$p(|y_1|, |y_2|) = p(|y_1|)p(|y_2|).$$

Therefore, (43) can be written into

$$\begin{aligned}
 P(|y|) &= \int_0^{|y|} \int_0^{|y|-|y_2|} p(|y_1|) p(|y_2|) d|y_1| d|y_2| \\
 &= \int_0^{|y|} \int_0^{|y|-|y_2|} \frac{|y_1|}{\Omega_1} \exp\left(-\frac{|y_1|^2}{2\Omega_1}\right) \\
 &\quad \frac{|y_2|}{\Omega_2} \exp\left(-\frac{|y_2|^2}{2\Omega_2}\right) d|y_1| d|y_2| \\
 &= 1 - \frac{\Omega_1}{\Omega_1 + \Omega_2} \exp\left(-\frac{|y|^2}{2\Omega_1}\right) \\
 &\quad - \frac{\Omega_2}{\Omega_1 + \Omega_2} \exp\left(-\frac{|y|^2}{2\Omega_2}\right) \\
 &\quad - \sqrt{\frac{\pi}{2}} \frac{1}{\Omega_1 + \Omega_2} \sqrt{\frac{\Omega_1 \Omega_2}{\Omega_1 + \Omega_2}} |y| \exp(-k|y|^2) \\
 &\quad \cdot \left(\operatorname{erf}(b) + \operatorname{erf}(a)\right)
 \end{aligned}$$

where

$$\begin{aligned}
 k &= \frac{1}{2(\Omega_1 + \Omega_2)}, \\
 b &= \frac{1}{\sqrt{2}} \sqrt{\frac{\Omega_1}{\Omega_2}} \frac{1}{\sqrt{\Omega_1 + \Omega_2}} |y|, \\
 a &= \frac{1}{\sqrt{2}} \sqrt{\frac{\Omega_2}{\Omega_1}} \frac{1}{\sqrt{\Omega_1 + \Omega_2}} |y|.
 \end{aligned}$$

The transformation of $|y|$ into γ is given in (28) as $\gamma = |y|^2 / (2\sigma_n^2)$. $P(|y|)$ can therefore be transformed into $P(\gamma)$ as follows:

$$\begin{aligned}
 P(\gamma) &= \Pr\left(\frac{|y|^2}{2\sigma_n^2} \leq \gamma\right) \\
 &= \Pr\left(|y| \leq \sqrt{2\sigma_n^2 \gamma}\right) \\
 &= p(|y|) \Big|_{|y|=\sqrt{2\sigma_n^2 \gamma}}. \quad (44)
 \end{aligned}$$

We can easily find that the final form of (44) is exactly (30).

Acknowledgements

This work has been performed in the ENIAC project ARTEMOS (Project No. 270683-2), in which the partner JKU is funded by the Austrian Research Promotion Agency (FFG) and the ENIAC Joint Undertaking.

References

- [1] PAULRAJ, A., GORE, D., NABAR, R., BOLCSKEI, H. An overview of MIMO communications – A key to gigabit wireless. *Proceedings of the IEEE*, 2004, vol. 92, no. 2, p. 198 - 218.
- [2] FOSCHINI, G. J., GANS, M. J. On limits of wireless communications in a fading environment when using multiple antennas. *Wireless Personal Communications*, 1998, vol. 6, p. 311 - 335.
- [3] PARSONS, J. D. *The Mobile Radio Propagation Channel*, 2nd Ed. Wiley, 2000.
- [4] BRENNAN, D. Linear diversity combining techniques. *Proceedings of the IEEE*, 2003, vol. 91, no. 2, p. 331 - 356.
- [5] DAMMANN, A., KAISER, S. Transmit/Receive-antenna diversity techniques for OFDM systems. *European Transactions on Telecommunications*, 2002, vol. 13, no. 5, p. 531 - 538.
- [6] HOEFEL, R. IEEE 802.11n: Performance analysis with spatial expansion, receive diversity and STBC. In *2012 IEEE Vehicular Technology Conference (VTC Fall)*. Quebec (Canada), 2012, p. 1 - 5.
- [7] HABIB, A., MEHLFUHRER, C., RUPP, M. Performance comparison of antenna selection algorithms in WiMAX with link adaptation. In *4th International Conference on Cognitive Radio Oriented Wireless Networks and Communications (CROWNCOM)*. Hannover (Germany), 2009, p. 1 - 5.
- [8] MEHTA, N. B., MOLISCH, A. F., ZHANG, J., BALA, E. Antenna selection training in MIMO-OFDM/OFDMA cellular systems. In *2nd IEEE International Workshop on Computational Advances in Multi-Sensor Adaptive Processing*. St. Thomas (VI, USA), 2007, p. 113 - 116.
- [9] PLICANIC, V., LAU, B. K., YING, Z. Performance of a multi-band diversity antenna with hand effects. In *International Workshop on Antenna Technology: Small Antennas and Novel Metamaterials (iWAT)*. Chiba (Japan), 2008, p. 534 - 537.
- [10] LINDBERG, P., KAIKKONEN, A., KOCHALI, B. Body loss measurements of internal terminal antennas in talk position using real human operator. In *International Workshop on Antenna Technology: Small Antennas and Novel Metamaterials (iWAT)*. China (Japan), 2008, p. 358 - 361.
- [11] PELOSI, M., FRANEK, O., KNUDSEN, M. B., CHRISTENSEN, M., PEDERSEN, G. F. A grip study for talk and data modes in mobile phones. *IEEE Transactions on Antennas and Propagation*, 2009, vol. 57, no. 4, p. 856 - 865.
- [12] MYLLYMAKI, S., HUTTUNEN, A., PALUKURU, V. K., JANTUNEN, H., BERG, M., SALONEN, E. T. Capacitive recognition of the users hand grip position in mobile handsets. *Progress In Electromagnetics Research B*, 2010, vol. 22, p. 203 - 220.
- [13] BERG, M., SONKKI, M., SALONEN, E. Absorption loss reduction in a mobile terminal with switchable monopole antennas. *IEEE Transactions on Antennas and Propagation*, 2011, vol. 59, no. 11, p. 4379 - 4383.
- [14] LAU, B. K., ANDERSEN, J., KRISTENSSON, G., MOLISCH, A. Impact of matching network on bandwidth of compact antenna arrays. *IEEE Transactions on Antennas and Propagation*, 2006, vol. 54, no. 11, p. 3225 - 3238.
- [15] GU, Q., DE LUIS, J., MORRIS, A., HILBERT, J. An analytical algorithm for pi-network impedance tuners. *IEEE Transactions on Circuits and Systems I: Regular Papers*, 2011, vol. 58, no. 12, p. 2894 - 2905.
- [16] HALPERN, S. The effect of having unequal branch gains practical predetection diversity systems for mobile radio. *IEEE Transactions on Vehicular Technology*, 1977, vol. 26, no. 1, p. 94 - 105.
- [17] OGAWA, K., MATSUYOSHI, T. An analysis of the performance of a handset diversity antenna influenced by head, hand, and shoulder effects at 900 MHz: Part I – Effective gain characteristics. *IEEE Transactions on Vehicular Technology*, 2001, vol. 50, no. 3, p. 830 - 844.

- [18] PAULRAJ, A., NABAR, R., GORE, D. *Introduction to Space-Time Wireless Communications*. Cambridge University Press, 2003.
- [19] OESTGES, C., CLERCKX, B. *MIMO Wireless Communications: From Real-World Propagation to Space-Time Code Design*. Boston (MA, USA): Elsevier, 2007.
- [20] VUCETIC, B., YUAN, J. *Space-Time Coding*. Wiley, 2003.
- [21] PROAKIS, J. G. *Digital communications*, 4th Ed. McGraw-Hill, 2000.
- [22] BIGLIERI, E. *MIMO Wireless Communications*. Cambridge (UK): Cambridge University Press, 2007.
- [23] LEE, W. C. Estimate of channel capacity in Rayleigh fading environment. *IEEE Transactions on Vehicular Technology*, 1990, vol. 39, no. 3, p. 187 - 189.
- [24] GÜNTHER, C. Comment on Estimate of channel capacity in Rayleigh fading environment. *IEEE Transactions on Vehicular Technology*, 1996, vol. 45, no. 2, p. 401 - 403.
- [25] SHANNON, C. E. A mathematical theory of communication. *The Bell System Technical Journal*, 1948, vol. 27, no. 3, p. 379 - 423.
- [26] LIU, P., SPRINGER, A. Impact of mobile antenna mismatch on receive antenna diversity in frequency-flat Rayleigh fading channels. In *2013 IEEE Vehicular Technology Conference (VTC Fall)*. Las Vegas (USA), 2013.

About Authors ...

Peng LIU was born in Mianyang, China. He received his Bachelor's degree in Mechanical Engineering and Automation from the University of Science and Technology Beijing (USTB) in 2006 and his Master's degree in Spacecraft Design from the Graduate University of the Chinese Academy of Sciences (GUCAS) in 2009. Currently he is a Ph.D. student at the Institute for Communications Engineering and RF-Systems (NTHFS) at Johannes Kepler University (JKU) Linz. Prior to joining NTHFS, he also worked on satellite communications for two years at the Academy of Opto-Electronics (AOE, an institution affiliated with the Chinese

Academy of Sciences) until June 2011. During 2007 and 2008, he mainly worked on high speed data processing and transfer. After that until 2011 he was dedicated to the design and implementation of a 300 Mbps high-data-rate receiver for space downlink communications. His research interests include MIMO, diversity techniques, antenna tuning/matching, software defined radio, digital signal processing.

Nemanja Stefan PEROVIĆ was born in Belgrade, Serbia. He received his Bachelor and Master degrees from the Faculty of Electrical Engineering, Belgrade University, Department of Electronics in 2008 and 2009 respectively. For a short time during 2010, he worked as an engineer for the Emission Technics part of the Radio Television of Serbia. Since 2011 he started his Ph.D. studies at the same university, Department of Telecommunications. Since 2013 he continues his Ph.D. studies at Johannes Kepler University (JKU) Linz, Institute for Communications Engineering and RF-Systems (NTHFS).

Andreas SPRINGER is a full professor and head of the Institute for Communications Engineering and RF-Systems (formerly Institute for Communications and Information Engineering) at the Johannes Kepler University Linz, Austria. In the Austrian Center of Competence in Mechatronics (ACCM) he serves as the coordinator for the research area Wireless Technologies. His current research interests are focused on wireless communication systems, single- and multi-carrier communications, architectures and algorithms for multi-band/multi-mode transceivers, UMTS/HSDPA/LTE, and recently wireless sensor networks. In these fields, he has published more than 180 papers in journals and at international conferences, one book, and two book chapters. In 2006 he was co-recipient of the science prize of the German Aerospace Center (DLR).